

## Original Article

# Aptamer-procalcitonin-antibody sandwich on an interdigitated microelectrode biosensor for diagnosing septic arthritis

Yan Jiang<sup>\*,a</sup>, Mei Lu<sup>†,b</sup>, Fanbo Pei<sup>\*,c</sup>

<sup>a</sup>Department of Intensive Care Unit, Yantai Hospital, Yantai, Shandong, China

<sup>b</sup>Department of Intensive Care Unit, Huaian Hospital of Huaian City, Huaian, Jiangsu, China

<sup>c</sup>Department of Emergency, Yang Ling Demonstration Zone Hospital, Xianyang, China

## ARTICLE INFO

### Keywords:

Aptamer  
Biomarker  
Biosensor  
Procalcitonin  
Septic arthritis

## ABSTRACT

Septic arthritis is a joint inflammation caused by an infectious etiology, mainly bacterial but occasionally by viral, mycobacterial, fungal, and other pathogens. Septic arthritis is monoarticular, affecting large joints, such as the knees or hip, and possibly causing severe joint destruction. In order to improve treatment and speed up healing, it is helpful to diagnose septic arthritis early. Early identification of septic arthritis is to provide timely medication and increase the recovery rate. Procalcitonin (PCT) has been proven to be a reliable marker for septic arthritis and has demonstrated diagnostic usefulness in the identification of bacterial infections. Here, a PCT biosensor was developed on a silica nanoparticle (SiNP)-modified interdigitated microelectrode (IDME). SiNP was modified on IDME by attaching it to an amine-linker and COOH-ended aptamer through the amine. SiNP-modified electrode increased the aptamer immobilization and was saturated at 800 nM. On the aptamer immobilized surfaces, PCT was quantified at values as low as 0.1 ng/mL [ $y = 4.103x - 7.0337$ ;  $R^2 = 0.9555$ ] by using anti-PCT antibody as a detection probe. Furthermore, PCT-spiked serum was detected from 0.1 ng/mL without any interference, and the control experiments with CTxII, CRP, and complementary aptamer failed to change the current responses, indicating the selective and specific identification of PCT.

## 1. Introduction

Septic arthritis is an infection in the joint tissues and joint (synovial) fluid. It is accompanied by inflammation, which is present in the synovial fluid that provides joints with lubrication, as well as the cartilage's surface [1]. The infection is typically bacterial, *Staphylococcus aureus* being the most common bacterial pathogen, but may also be viral, mycobacterial, fungal, or other unusual pathogens [2]. The infection normally originates from another body part due to an injury, surgery, or injection and then proceeds to travel through the bloodstream to reach the joints [3]. While it is more common for larger joints, such as the knees or hips, to be affected due to the monoarticular nature of septic arthritis, polyarticular septic arthritis may also arise in smaller joints, such as the ankles or shoulders. Septic arthritis is associated with mortality and morbidity with symptoms such as quick joint destruction, inflammatory response, and swelling [4]. In the United States, there is a disease incidence of 4-60 cases per 100,000 patients annually, which increases to 70 cases per 100,000 patients per year for immunocompromised patients. Mortality rates may also be substantial, as they range from 3-25% [5]. While the disease has severe characteristics, it may present a patient with symptoms that can range from subtle to life-threatening, which heightens the chances of patients missing typical symptoms or signs. There is also the issue of multiple other conditions possessing similar characteristics and symptoms to

septic arthritis, creating difficulty in diagnosis [2]. Therefore, it is urgent to develop a biosensor for the diagnosis of early stages of septic arthritis.

Biosensors are analytical devices that allow the measurement of chemical or biological reactions through the generation of signals proportional to an analyte's concentration in a reaction [6,7]. This property causes them to show high potential in healthcare diagnostics for functions such as disease-causing micro-organization detection, disease monitoring, and drug discovery [8]. A biosensor typically consists of three main components: analyte, bioreceptor, and transducer. The analyte is the subject of detection, the bioreceptor is a molecule made to recognize the analyte, and the transducer is a component that allows the conversion of a bio-recognition event into a signal that can be measured [9,10]. Bioreceptors are normally DNA molecules, aptamers, or enzymes, while transducers may be electrochemical, mass, or optical materials [10,11]. Nanomaterials, which consist of nanoparticles that are at least one dimension less than 100 nm, are being explored for their application in biosensor diagnostic devices [12]. They are specifically used as materials for transducers, a significant part of the development of biosensors [13-15]. This is due to the desirable properties of nanomaterials, which include their compatibility with biological molecules, ability to amplify signals, nanoscale size, and high electrical conductivity [16]. It has also been discovered that the incorporation of nanomaterials opens the possibility of improved biosensor performance

### \*Corresponding author:

E-mail address: pfb093897@outlook.com (F. Pei)

†Authors contributed equally to this work and shared co-first authorship.

Received: 15 January, 2025 Accepted: 11 March, 2025 Epub Ahead of Print: 16 April 2025 Published: \*\*\*

DOI: 10.25259/AJC\_43\_2025

due to the lower limit of detection of multiple orders of magnitudes as well as the improved sensitivities [17,18]. This is due to nanomaterials providing a platform for customization and manipulation, in which researchers are allowed to tune properties to the smallest detail for the purpose of matching diverse biosensing application requirements [19]. This, thus, allows biosensors to possess greater selectivity, performance, and sensitivity.

These nanomaterial-based biosensors may be applied for septic arthritis diagnosis. Currently, septic arthritis is diagnosed through radiological and clinical tests, including Magnetic resonance imaging (MRI), computerized tomography (CT), and X-ray [20]. The analysis of aspirated synovial fluid and serum inflammatory markers is necessary for diagnosis confirmation. The process takes time, and the amalgamation of clinical techniques and features does not allow accurate information about the presence of certain microorganisms to be accurate. Nanomaterials have the greatest potential for the management of diagnosis of septic arthritis. In this research, silica nanoparticles (SiNP) were separated from rice husk ash and used for surface modification to identify procalcitonin (PCT), which is a well-known biomarker for septic arthritis.

PCT is produced by neuroendocrine cells of the thyroid and is converted into calcitonin, so it does not enter the blood circulation. Hence, the level of PCT in a healthy person's serum is less than 0.05 ng/mL [21]. This level is increased drastically with bacterial infection and inflammatory response. Depending on sepsis severity, the values increase between 10 and 100 ng/mL. Slightly elevated levels of PCT (between 0.05 and 0.5 ng/mL) are noted as a localized infection [22]. In addition, PCT shows a rapid rise in the blood serum within 2-6 hrs of acute infection, quantifying the level of PCT helps identify the bacterial infection and inflammatory condition. Apart from that, the level of PCT helps to differentiate between non-septic and septic arthritis in people with joint inflammation. It is, thus, a specific and sensitive biomarker for septic arthritis [23]. This research quantifies the level of PCT on a SiNP-modified interdigitated microelectrode (IDME) surface by utilizing aptamer and antibody as the capturing and detection probes, respectively. IDME has been demonstrated widely as a dielectrode system, with different designs. The popular designs are parallel and interdigitated patterns, as well as concentric patterns with uniform gaps. The successful sizes for gaps and electrodes are at microscale ranges. These kinds of electrode systems can be operated at low power on a dual probe station for a high-performance analysis. IDME works by causing a dipole moment between dual electrodes connected between positive- and negative-electrodes. The dipole moment occurs due to the movement of ions between two electrodes, and these ionic movements, changing with surface measurements or surface molecular interactions, are measured.

## 2. Materials and Methods

### 2.1. Reagents and biomolecules

(3-Aminopropyl)triethoxysilane (APTMS), PEG-COOH, PCT, Phosphate buffered saline (PBS), anti-PCT antibody, and human serum were bought from Sigma-Aldrich (USA). IDME was synthesized as described previously [24]. COOH ended aptamer (5'-COOH-CCGCGGCA GTTCCGTAATGTTAATGCCTATACTTGAGCTG-3') and complementary aptamer (5'-COOH-GGCGCCGTCAAGGCATTACAATTACGGATATGA ACTCGAC-3') sequences were synthesized and received from Apical Scientific, Malaysia [23]. On IDME, the power supply was provided by a pico ammeter on a dual power station at the range between 0 and 2 Volts and measured with the intervals of 0.1 V. All measurements were performed at room temperature (RT) and the sensing surface was maintained wet using 10 mM Phosphate-buffered saline (PBS) (pH 7.4). Washings were carried out using the same buffer, between each surface modification or interaction using a 10-reaction volume. To maintain consistency in the measurements, washing was performed on a probe station without disturbing the electrodes.

### 2.2. Extraction of potassium silicate from rice husk ash

The rice husk was first burned for six hrs at 500°C to eliminate the hydrocarbons, after which it was soaked in 10 M of HCl for a day to

eliminate any extraneous minerals except for silica. After treating the resulting ash with 10% HCl and heating it for 3 hrs at 100°C while stirring to remove any impurities, it was rinsed with distilled water to bring its pH down to 7. Subsequently, the refined ash was dried for three hrs at 100°C. About 30 g of ash was blended with 10 M of KOH and heated at 300°C for 3 hrs to extract the potassium silicate solution ( $K_2SiO_3$ ). After 3 hrs, the potassium silicate solution was collected through a Whatman filter paper (pore size=0.7  $\mu$ m).

### 2.3. Preparation of silica nanopowder from potassium silicate solution

Silica nanopowder was prepared by using the extracted  $K_2SiO_3$  from the rice husk ash. For this process, 250 mL of  $K_2SiO_3$  was added to 250 mL of distilled water and then 10% of HCl was introduced dropwise until the pH reached 7, white gel formation was noted at this point. The gel was then stirred overnight to get a uniform distribution of the silica nanopowder. To obtain the powder form of silica, the gel was dried at 100°C for 16 hrs, separated by centrifugation, and cleaned with distilled water the next day.

### 2.4. Creating an amine linker on the surface of silica nanopowder

Amine was linked with SiNP for the surface functionalization process. Briefly, 1  $\mu$ L APTMS (2% dissolved in 30% ethanol) was mixed with 1 mg/mL of SNP, and the mixture was shaken for 3 hrs. Following that, centrifugation was used to collect the altered nanoparticle and wash it in 30% ethanol. In preparation for additional modification, the isolated amine-modified SiNP complex was dried at room temperature (RT).

### 2.5. Optimizing aptamer immobilization on SiNP

Anti-PCT aptamer was modified on the IDME through the amine-modified SiNP. Since aptamer immobilization plays a major role in PCT detection, aptamer was diluted to 100 to 1600 nM, and the immobilization efficiency was optimized. For this process, IDME was initially dipped in KOH (1%) solution for the hydroxylation process, and then amine-modified SiNP was placed and rested for 3 hrs. After that, the excess amine was removed by washing the surface with diluted ethanol. Furthermore, COOH-ended aptamer with 100 nM was introduced to the SiNP-modified amine surface. The surface current was recorded after washing the surface with PBS. Similarly, other concentrations of aptamer (200 to 1600 nM) were attached to the electrode. The current measurements were analyzed, and the suitable aptamer concentration for PCT detection was determined.

### 2.6. Optimizing of anti-procalcitonin antibody

Antibody was used as the detection probe in the PCT biosensor. To identify the necessary antibody concentration, antibodies from 50 to 400 nM were optimized. For this process, the same process was followed until the aptamer immobilization. PEG-COOH was used to block the excess amine surface, followed by the introduction of 1 nM PCT, and then it was rested for 30 mins. Finally, 50 nM antibody was added and it was rested for another 30 mins. The surface current was recorded after washing the surface with PBS. The same experiment was conducted for other antibody concentrations (100, 200, and 400 nM).

### 2.7. Detection of PCT by aptamer and antibody

PCT was detected on SiNP-modified IDME. The steps involved in this process are as follows: (i) IDME was immersed in KOH for 10 mins; (ii) SiNP-APTMS was added and it was rested for 3 hrs; (iii) Aptamer was introduced for 30 mins; (iv) PEG-COOH was placed on the electrode for 30 mins; (v) PCT (0.01 to 20 ng/mL) was added for 30 mins; (vi) Optimized PCT antibody was dropped and kept for 30 mins. In between each step, the surface was washed with PBS and then the current was measured to identify PCT-binding with its antibody and aptamer.

### 2.8. Selective and specific detection of procalcitonin

Selective identification of PCT (0.01 to 20 ng/mL) was performed with PCT dissolved in human serum. PCT was diluted in human serum

and detected by aptamer-PCT-antibody sandwich assay. All other experimental conditions and the concentrations of biomolecules were kept constant. Specific performances with control proteins, namely CRP, and CTxII, and complementary aptamer, were conducted. Four different experiments were performed (i) CRP instead of PCT; (ii) CTxII instead of PCT; (iii) complementary aptamer instead of specific aptamer; and (iv) IgG antibody instead of anti-PCT antibody. The 20 ng/mL CRP and CTxII concentrations were dropped on the aptamer and sandwiched with the antibody. In another experiment, PCT was allowed to interact with the complementary aptamer-attached surfaces and then sandwiched with the antibody. The current measurements were recorded for all the control experiments and compared with three specific PCT detections.

### 3. Results and Discussion

Septic arthritis, an orthopedic emergency, can seriously harm the joints and raise morbidity and death rates. Early detection of the infection facilitates more effective therapy and accelerates the healing process for septic arthritis. Herein, a PCT biosensor was developed on a SiNP-modified IDME by utilizing the molecules, aptamer, and antibody as the capturing and detection probes, respectively. Figure 1(a) and 1(b) shows graphical representation of the PCT biosensor. KOH-treated IDME was converted into APTMS-SiNP through the interaction of KOH with APTMS. Further, an aptamer ending with COOH was added. COOH bound with the amine in the APTMS, and then PEG-COOH was added as the blocking molecule to suppress the nonspecific binding. PEG-COOH was used to block the amine surface of APTMS. In general, amine-modified surfaces attract other biomolecules electrostatically, which leads to a false positive signal. To reduce the biofouling, PEG-COOH was utilized, which can bind the excess amine surfaces and reduce the signal-to-noise ratio. After that, PCT was added, anti-PCT antibody interacted. In this surface modification, aptamer was used to capture PCT. The aptamer is an artificial antibody, having more positive features than the antibody, such as higher selectivity, sensitivity, low-cost, no batch variation, easy modification, and flexibility for surface functionalization [24,25]. Since aptamer is more specific for its target, it attracts only the specific molecule when used as the capturing probe. This improves the specific detection of PCT and lowers the detection limit because the aptamer's binding affinity is higher with the target than the antibody. So, an aptamer was designed to capture PCT and then detect it using an antibody. [18,26,27]. Apart from that, SiNP was utilized to improve the aptamer's binding on IDME. Since the surface of the SiNP was covered with APTMS, it could attract a higher number of COOH-ended aptamers. It was proved that SiNP-modified biomolecules are stable on the electrode and enhance the biomolecular interactions.

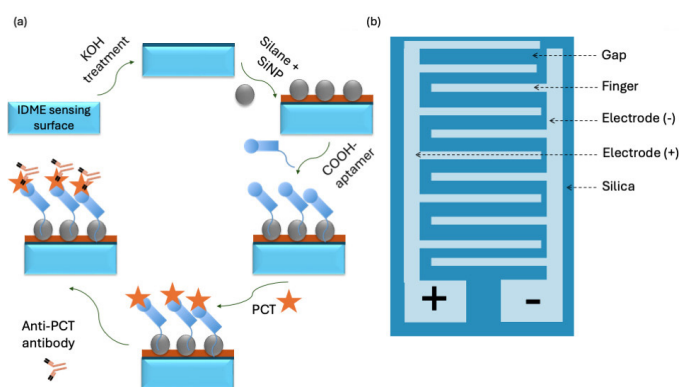


**Figure 1.** (a) Graphical representation of PCT biosensor. KOH-treated IDME was modified into APTMS-SiNP. Further, an aptamer end with COOH was added. PEG-COOH was added to suppress the nonspecific binding. After that, PCT was added, followed by anti-PCT antibody. (b) Surface structure of IDME. Electrodes and gaps are indicated. PCT: Procalcitonin, IDME: interdigitated microelectrode, APTMS-SiNP: (3-Aminopropyl) triethoxysilane-silica nanoparticle.

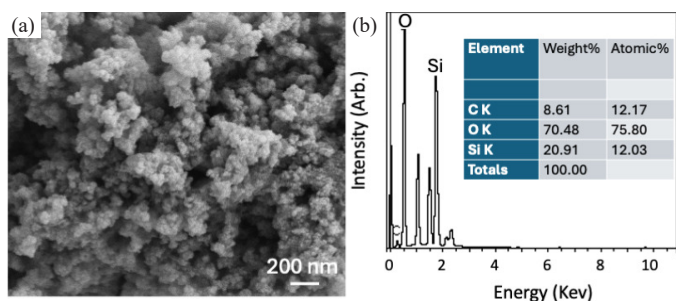


**Figure 2.** (a) FESEM image of SiNP revealing a homogeneous distribution of SiNP with no sign of agglomeration, an average size of SiNP is around  $30 \pm 10$  nm. (b) EDX results show that the major elements Si (20.9%), O (70.4%), and C (8.6%) were found in the isolated SiNP, confirming the synthesis of SiNP from the rice husk ash. EDX: Energy dispersive X-ray spectroscopy, FESEM: Field emission scanning electron microscopy SiNP: silica nanoparticle.

#### 3.1. Nanoscale imaging of SiNP

Field emission scanning electron microscopy (FESEM) was used to analyze the size and shape of SiNP extracted from the rice husk ash. The FESEM image revealed a homogeneous distribution of SiNP with no sign of agglomeration (Figure 2a); the average size of an SiNP is around  $30 \pm 10$  nm. EDX results show that elements majorly found in the SiNP were Si (20.9%), O (70.4%), and C (8.6%), confirming the synthesis of SiNP from rice husk ash (Figure 2b).

#### 3.2. Aptamer concentration optimization

Since aptamer attachment on the electrode plays a major role in improving the PCT biosensor, different aptamer concentrations were tested on the SiNP-modified IDME. Maximum amount of aptamer immobilization attracts more PCT and improves the analytical performances. Figure 3(a) shows the current-volt graph of different aptamer concentrations binding on APTMS-SiNP. As shown in the figure, KOH-treated IDME showed a current level of  $6.75 \times 10^{-11}$  A, and after modifying the surface into APTMS-SiNP, the surface current increased to  $4.06 \times 10^{-10}$  A. These current changes indicated that the electrode was modified into SiNP. Further addition of 100 nM aptamer increased the current to  $7.65 \times 10^{-10}$  A, which confirms aptamer attachment on APTMS-SiNP. Increasing the aptamer concentration (200, 400, 800, and 1600 nM), increased the current levels ( $1.46 \times 10^{-9}$  A,  $2.05 \times 10^{-9}$  A,  $2.46 \times 10^{-9}$  A, and  $2.53 \times 10^{-9}$  A, respectively) (Figure 3b). The response of current was saturated from 800 nM, which means that 800 nM of aptamer is enough to completely cover the APTMS-SiNP. Increasing aptamer concentration further leaves no space to attach to the sensing electrode, and the excess gets washed out during the washing process. Apart from that, PCT was quantified in the range of 0.01 to 1 ng/mL, and 800 nM of aptamer was enough to attract the highest concentration of PCT (1 ng/mL). We optimized 800 nM of aptamer for the PCT sandwich assay.

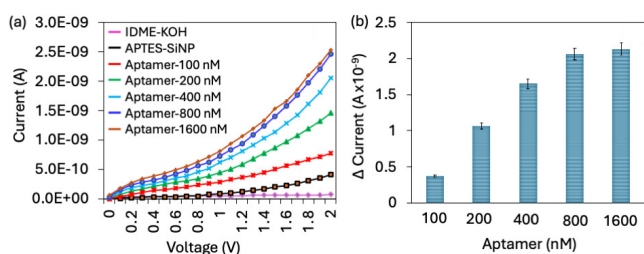


**Figure 3.** Aptamer optimization. (a) Current-volt measurement of different aptamer concentrations binding on APTMS-SiNP. The current level was increased for each concentration of aptamer. (b) The current response of aptamer immobilization. With increasing the aptamer, the current response also increased, it was saturated from 800 nM. All experiments were performed as triplicates on different devices fabricated from the same batch, and data were averaged. APTMS-SiNP: (3-Aminopropyl)triethoxysilane-silica nanoparticle.

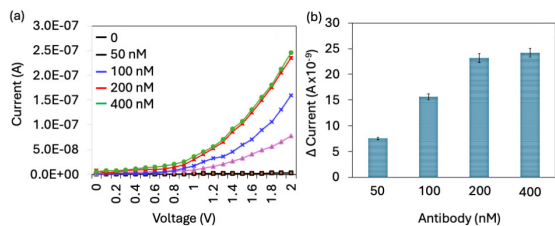


**Figure 4.** Antibody optimization. (a) Current-volt graph of different antibody concentrations binding on PCT immobilized surface. Current was increased for each concentration of antibody. (b) Current response of antibody immobilization. With increasing the antibody, current response also increased; it was saturated from 200 nM. All experiments were performed as triplicates on different devices fabricated from the same batch, and data were averaged. PCT: Procalcitonin.

### 3.3. Optimizing anti-PCT antibody

After aptamer optimization, the anti-PCT antibody was optimized to improve PCT biosensing. Antibody was used as a detection molecule in the aptamer-PCT-antibody sandwich assay. The necessary amount of antibody is needed to detect the immobilized PCT on the aptamer-modified surfaces. For this process, antibody concentrations of 50 to 200 nM were optimized with a fixed aptamer and PCT concentration (Figure 4a). Without antibody, the current response was noted as 2.53 E-09 A; after adding 50 nM the current was slightly increased to 2.76 E-09 A, which means the antibody was not enough for complete binding with PCT. Increasing the antibody concentrations to 100, 200, 400, and 800 nM, changed the current levels to 7.78 E-08 A, 1.59 E-07 A, 2.35 E-07 A, and 2.45 E-07 A, respectively. After adding 100 nM antibody, the current drastically increased until the 400 nM antibody concentration. After that there was no increment of current response (Figure 4b). This means that 400 nM of antibody was enough to maximise the current response for 1 nM of PCT. So, 400 nM of antibody was optimized for the aptamer-PCT-antibody sandwich assay to enhance the biomolecular interaction and lower the detection limit of PCT.

### 3.4. Quantification of procalcitonin

PCT was quantified on an SiNP-modified IDME using an aptamer and antibody sandwich assay. On the aptamer attached surfaces, different concentrations of PCT (0.01 to 20 ng/mL) were added, and the anti-PCT antibody was interacted. As shown in Figure 5(a), before adding PCT, the current response was recorded at 2.46 E-09A, and after adding 0.01 ng/mL of PCT, the current slightly increased to 2.76 E-09A. There was no significant difference in current with 0.01 ng/mL of PCT. With a further increment of PCT to 0.1 ng/mL, the current level was increased from 2.46 to 5.18 E-09 A. The current response almost doubled at PCT concentration of 0.1 ng/mL (Figure 5b). With increase in the PCT concentration to 1, 5, 10, 15, and 20 ng/mL, current levels increased to 3.45 E-08 A, 7.91 E-08 A, 1.3 E-07 A, 1.87 E-07 A, and 2.35 E-07 A, respectively. It was noticed that 1 ng/mL showed a higher jump of current responses and constant increment. This higher level of current response was achieved by higher immobilization of the aptamer

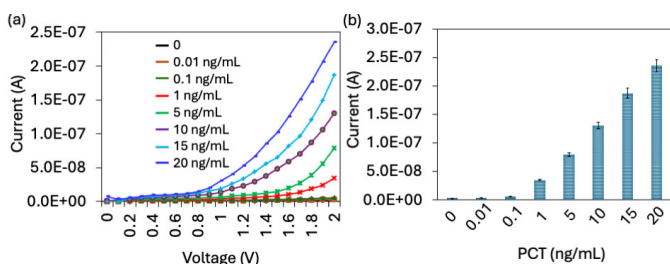


**Figure 5.** (a) Quantification of PCT. Current-volt graph for different concentrations of PCT detection by aptamer-PCT-antibody. Current level was increased for each concentration of PCT. (b) Current response of PCT detection. There is no significant difference in current response was noted with 0.01 ng/mL of PCT. From 0.1 ng/mL, a clear increment of current was noted. All experiments were performed as triplicates on different devices fabricated from the same batch, and data were averaged. PCT: Procalcitonin.

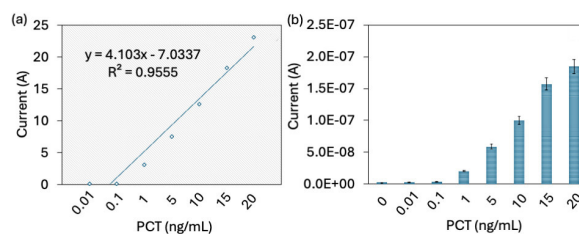


**Figure 6.** (a) Limit of detection of PCT. The difference in current for each PCT was calculated, plotted in an Excel spreadsheet, and the limit of detection of PCT was 0.1 ng/mL with an  $R^2$  value of 0.9555. (b) PCT detection in target spiked serum sample. Current response was increased with increasing PCT without any interference. All experiments were performed as triplicates on different devices fabricated from the same batch and data was averaged. PCT: Procalcitonin.

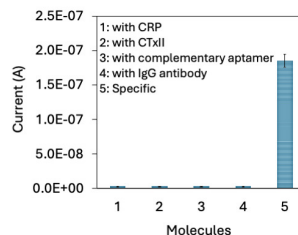


**Figure 7.** Specific PCT detection was further analyzed with control proteins, namely CRP and CTxII, and with complementary aptamer. There is no notable difference of current was recorded with control molecules. All experiments were performed as triplicates on different devices fabricated from the same batch, and data were averaged. CRP: C-reactive protein, CTxII: C-terminal cross-linked telopeptides of type II collagen. PCT: Procalcitonin.

through the SiNP on IDME. APTMS-modified SiNP attracts a higher number of COOH-ended aptamers and provides a better stability and orientation on the IDME, which helps to attract higher PCT and further increases the current response. Various research proved that silica is stable, biocompatible, and simple to functionalize with biomolecules [28]. In addition, SiNPs' enormous surface area and capacity for functionalization enable them to detect target analytes at very low concentrations [29]. Biomarkers conjugated with SiNPs are used to detect various diseases such as cancer, diabetes, and infectious diseases [30]. Here SiNPs were utilized to improve aptamer attachment on IDME, which enhanced the analytical performances for PCT, with its aptamer and antibody. The difference in current for each PCT was calculated and plotted in an Excel spreadsheet, and the limit of detection of PCT was calculated as 0.1 ng/mL with an  $R^2$  value of 0.9555 (Figure 6a).

### 3.5. Selective and specific detection of PCT

For the selective identification of PCT (0.01 to 20 ng/mL), PCT was dissolved in the human serum and detected by the aptamer-PCT-antibody sandwich assay. As shown in Figure 6(b), the current response was increased with increasing PCT without any interference. Research has found that the cutoff value of PCT in human serum is around 0.25 ng/mL and it is increased when people have septic arthritis. The serum PCT cutoff was found at 0.25 ng/mL and determined as the diagnosis marker for septic arthritis. Another research found that serum PCT values at 0.5 ng/mL are an accurate biomarker for pyogenic infections [1]. In addition, it was proved that the serum PCT would be superior to other biomarkers, which include CRP, ESR, and WBC at discerning septic arthritis from aseptic arthritis [31]. Our sensing system identified the PCT level in the serum spiked sample from 0.1 ng/mL without any interference helps to diagnose the septic arthritis and its conditions. Specific PCT detection was further analyzed with control proteins, namely CRP and CTxII, and with a complementary aptamer. Four different experiments were performed: (i) CRP instead of PCT, (ii) CTxII instead of PCT, (iii) complementary aptamer instead of aptamer, and (iv) IgG antibody instead of anti-PCT antibody. As shown in Figure 7, there was no notable difference in current with control molecules compared with specific experiment indicating the specific detection of PCT.

#### 4. Conclusions

Septic arthritis is a serious joint infection caused by microorganisms, particularly bacteria. It causes excruciating joint pain and edema surrounding the joint. Severe and untreated infection leads to serious health issues. Diagnosing septic arthritis at the initial stages helps to provide the necessary treatment. PCT is known as a specific and efficient blood-based biomarkers for septic arthritis. This research was focused to develop a PCT biosensor on an IDME modified with SiNPs. The aptamer was attached to SiNP through an amine-COOH linker, and it was saturated at 800 nM. On the aptamer-attached electrodes, PCT was quantified as low as 0.1 ng/mL by an aptamer-PCT-antibody sandwich. Selective experiments with PCT-spiked serum show an increasing trend of current responses, and with the control molecules, the current responses are constant, indicating the selective and specific detection of PCT. This SiNP-modified sensor identified the lower level of PCT and diagnosed septic arthritis. The current research has demonstrated good performance; however, when changing the surface with different nanomaterials, it needs fine-tuning to provide optimal conditions. Further, sensitivity may vary depending on the affinity between the interactive molecules.

#### CRedit authorship contribution statement

**Yan Jiang and Mei Lu:** Data curation, Formal analysis, Investigation, Writing original draft preparation, **Fenbo Pei:** Methodology, Conceptualization, Project administration, Funding acquisition, Resources, Writing-Reviewing and Editing, All authors have read and agreed with the content of manuscript.

#### Declaration of competing interest

The authors declare no competing interest.

#### Declaration of generative AI and AI-assisted technologies in the writing process

The authors confirm that there was no use of artificial intelligence (AI)-assisted technology for assisting in the writing or editing of the manuscript and no images were manipulated using AI.

#### References

- Maharajan, K., Patro, D.K., Menon, J., Hariharan, A.P., Parija, S.C., Poduval, M., Thimmaiah, S., 2013. Serum procalcitonin is a sensitive and specific marker in the diagnosis of septic arthritis and acute osteomyelitis. *Journal of Orthopaedic Surgery and Research*, **8**, 19. <https://doi.org/10.1186/1749-799X-8-19>
- Wang, J., Wang, L., 2021. Novel therapeutic interventions towards improved management of septic arthritis. *BMC Musculoskeletal Disorders*, **22**, 530. <https://doi.org/10.1186/s12891-021-04383-6>
- Donders, C.M., Spaans, A.J., van Wering, H., van Bergen, C.J., 2022. Developments in diagnosis and treatment of paediatric septic arthritis. *World Journal of Orthopedics*, **13**, 122-130. <https://doi.org/10.5312/wjo.v13.i2.122>
- Tzani, P., Klavdianou, K., Lazarini, A., Theotikos, E., Balanika, A., Fanouriakos, A., Elezoglou, A., 2022. Septic arthritis complicating a gout flare: Report of two cases and review of the literature. *Mediterranean Journal of Rheumatology*, **33**, 75-80. <https://doi.org/10.31138/mjr.33.1.75>
- Long, B., Koyfman, A., Gottlieb, M., 2019. Evaluation and management of septic arthritis and its mimics in the emergency department. *The Western Journal of Emergency Medicine*, **20**, 331-341. <https://doi.org/10.5811/westjem.2018.10.40974>
- Qin, D., Gong, Q., Li, X., Gao, Y., Gopinath, S.C.B., Chen, Y., Yang, Z., 2023. Identification of mycoplasma pneumoniae by DNA-modified gold nanomaterials in a colorimetric assay. *Biotechnology and Applied Biochemistry*, **70**, 553-9. <https://doi.org/10.1002/bab.2377>
- Anasass, J.R., Kannaiyan, P., Gopinath, S.C.B., 2022. Biosynthesis of zerovalent iron nanoparticles for catalytic reduction of 4-nitrophenol and decoloration of textile dyes. *Biotechnology and Applied Biochemistry*, **69**, 2780-2793. <https://doi.org/10.1002/bab.2323>
- Gopinath, N., 2023. Artificial intelligence and neuroscience: An update on fascinating relationships. *Process Biochemistry*, **125**, 113-120. <https://doi.org/10.1016/j.procbio.2022.12.011>
- LakshmiPriya, T., Hashim, U., Gopinath, S.C.B., Azizah, N., 2016. Microfluidic-based biosensor: Signal enhancement by gold nanoparticle. *Microsystem Technologies*, **22**, 2389-2395. <https://doi.org/10.1007/s00542-016-3074-1>
- LakshmiPriya, T., Horiguchi, Y., Nagasaki, Y., 2014. Co-immobilized poly(ethylene glycol)-block-polyamines promote sensitivity and restrict biofouling on gold sensor surface for detecting factor IX in human plasma. *The Analyst*, **139**, 3977-3985. <https://doi.org/10.1039/c4an00168k>
- Gopinath, S.C., Tang, T.H., Citartan, M., Chen, Y., LakshmiPriya, T., 2014. Current aspects in immunosensors. *Biosensors & Bioelectronics*, **57**, 292-302. <https://doi.org/10.1016/j.bios.2014.02.029>
- LakshmiPriya, T., Fujimaki, M., Gopinath, S.C., Awazu, K., Horiguchi, Y., Nagasaki, Y., 2013. A high-performance waveguide-mode biosensor for detection of factor IX using PEG-based blocking agents to suppress non-specific binding and improve sensitivity. *The Analyst*, **138**, 2863-2870. <https://doi.org/10.1039/c3an00298e>
- Taniselass, S., Arshad, M.K.M., Gopinath, S.C.B., 2019. Graphene-based electrochemical biosensors for monitoring noncommunicable disease biomarkers. *Biosensors & Bioelectronics*, **130**, 276-292. <https://doi.org/10.1016/j.bios.2019.01.047>
- Taguchi, M., Ptityn, A., McLamore, E.S., Claussen, J.C., 2014. Nanomaterial-mediated biosensors for monitoring glucose. *Journal of Diabetes Science and Technology*, **8**, 403-411. <https://doi.org/10.1177/1932296814522799>
- Zhao, F., Wu, J., Ying, Y., She, Y., Wang, J., Ping, J., 2018. Carbon nanomaterial-enabled pesticide biosensors: Design strategy, biosensing mechanism, and practical application. *TrAC Trends in Analytical Chemistry*, **106**, 62-83. <https://doi.org/10.1016/j.trac.2018.06.017>
- Jo, H.J., Kang, M.S., Jang, H.J., Raja, I.S., Lim, D., Kim, B., Han, D.-W., 2023. Advanced approaches with combination of 2D nanomaterials and 3D printing for exquisite neural tissue engineering. *Materials Science in Additive Manufacturing*, **2**, 0620. <https://doi.org/10.36922/msam.0620>
- Yun, Y.H., Eteshola, E., Bhattacharya, A., Dong, Z., Shim, J.S., Conforti, L., Kim, D., Schulz, M.J., Ahn, C.H., Watts, N., 2009. Tiny medicine: Nanomaterial-based biosensors. *Sensors (Basel, Switzerland)*, **9**, 9275-9299. <https://doi.org/10.3390/s91109275>
- Geng, H., Gopinath, S.C.B., Niu, W., 2022. Highly sensitive Hepatitis B virus identification by antibody-aptamer sandwich enzyme-linked immunosorbent assay. *INNOVOC Therapeutics and Pharmacological Sciences*, **5**, 7-14. <https://doi.org/10.36922/itps.298>
- Jiang, C., Lan, L., Yao, Y., Zhao, F., Ping, J., 2018. Recent progress in application of nanomaterial-enabled biosensors for ochratoxin A detection. *TrAC Trends in Analytical Chemistry*, **102**, 236-249. <https://doi.org/10.1016/j.trac.2018.02.007>
- Bozza, F.A., Garteiser, P., Oliveira, M.F., Doblas, S., Cranford, R., Saunders, D., Jones, I., Townner, R.A., Castro-Faria-Neto, H.C., 2010. Sepsis-associated encephalopathy: A magnetic resonance imaging and spectroscopy study. *Journal of Cerebral Blood Flow & Metabolism*, **30**, 440-8. <https://doi.org/10.1038/jcbfm.2009.215>
- Morgenthaler, N.G., Struck, J., Fischer-Schulz, C., Seidel-Mueller, E., Beier, W., Bergmann, A., 2002. Detection of procalcitonin (PCT) in healthy controls and patients with local infection by a sensitive ILMA. *Clinical Laboratory*, **48**, 263-270.
- Pavic, M., Bronic, A., Milevoj Kopcinovic, L., 2010. Procalcitonin in systemic and localized bacterial infection. *Biochemia Medica*, 236-241. <https://doi.org/10.11613/bm.2010.029>
- Park, D.-Y., Shin, W.-R., Kim, S.Y., Nguyen, Q.-T., Lee, J.-P., Kim, D.-Y., Ahn, J.-Y., Kim, Y.-H., 2023. In silico molecular docking validation of procalcitonin-binding aptamer and sepsis diagnosis. *Molecular & Cellular Toxicology*, **19**, 843-855. <https://doi.org/10.1007/s13273-023-00384-9>
- Liu, L., Gopinath, S.C.B., Wu, Y.S., Zhao, W., 2022. Gold-enhanced current-volt dielectrode junction for biosensing with an aptamer-insulin-like growth factor-1-antibody sandwich pattern. *Materials Express*, **12**, 464-471. <https://doi.org/10.1166/mex.2022.2153>
- Luo, J., Gopinath, S.C.B., Subramaniam, S., Wu, Z., 2022. Arthritis biosensing: Aptamer-antibody-mediated identification of biomarkers by ELISA. *Process Biochemistry*, **121**, 396-402. <https://doi.org/10.1016/j.procbio.2022.07.022>
- Wang, F., Gopinath, S.C., LakshmiPriya, T., 2019. Aptamer-antibody complementation on multiwalled carbon nanotube-gold transduced dielectrode surfaces to detect pandemic swine influenza virus. *International Journal of Nanomedicine*, **14**, 8469-8481. <https://doi.org/10.2147/IJN.S219976>
- Ocaña, C., Hayat, A., Mishra, R., Vasilescu, A., del Valle, M., Marty, J.L., 2015. A novel electrochemical aptamer-antibody sandwich assay for lysozyme detection. *The Analyst*, **140**, 4148-4153. <https://doi.org/10.1039/c5an00243e>
- Prabha, S., Durgalakshmi, D., Rajendran, S., Lichtfouse, E., 2021. Plant-derived silica nanoparticles and composites for biosensors, bioimaging, drug delivery and supercapacitors: A review. *Environmental Chemistry Letters*, **19**, 1667-1691. <https://doi.org/10.1007/s10311-020-01123-5>
- Kell, A.J., Pagé, L., Tan, S., Charlebois, I., Boissinot, M., Leclerc, M., Simard, B., 2011. The development of a silica nanoparticle-based label-free DNA biosensor. *Nanoscale*, **3**, 3747-3754. <https://doi.org/10.1039/c1nr10435g>
- Mathelié-Guinlet, M., Gammoudi, I., Beven, L., Moroté, F., Delville, M.-H.élène, Grauby-Heywang, C., Cohen-Bouhacina, T., 2016. Silica nanoparticles assisted electrochemical biosensor for the detection and degradation of escherichia coli bacteria. *Procedia Engineering*, **168**, 1048-1051. <https://doi.org/10.1016/j.proeng.2016.11.337>
- Hügler, T., Schuetz, P., Mueller, B., Laifer, G., Tyndall, A., Regenass, S., Daikeler, T., 2008. Serum procalcitonin for discrimination between septic and non-septic arthritis. *Clinical and Experimental Rheumatology*, **26**, 453-6. PMID: 18578968.